Crustal contribution in the genesis of the bimodal Triassic volcanism from the Coastal Range, central Chile

Diego Morata

Luis Aguirre

Departamento de Geología, Facultad de Ciencias Físicas y Matemáticas, Universidad de Chile, Casilla 13518, Correo 21, Santiago, Chile

Marcela Oyarzún

dmorata@cec.uchile.cl

Mario Vergara

ABSTRACT

Triassic volcanism in the Coastal Range of central Chile is represented by the Pichidangui Formation (31°54' to 32°15'S) composed of acid and basic lava flows and sub-volcanic intrusives with some sedimentary intercalations. Both rock types have been affected by non-deformational very low- to low-grade metamorphism. Their geochemical characteristics indicate a tholeiitic affinity, with Nb/Y ratios ranging from 0.20-0.17. Low [mg] values in the basic rocks are indicative of non-primitive liquids. Differences in immobile trace element and REE (LREE/HREE, Eu/Eu*) between basic and acid rocks are consistent with their isotopic signature, with initial ratios of $(^{87}Sr/^{86}Sr)_o$ and $(^{143}Nd/^{144}Nd)_o$ ranging from 0.70397 to 0.70597 and from 0.512515 to 0.512608 respectively in the basic rocks, and from 0.70514-0.71161 to 0.512108-0.512526 respectively in the acid rocks. These chemical and isotopic differences between both types of magmatism are interpreted as a consequence of different degrees of crustal contamination from an enriched mantle source with a lithospheric component in an extensional intracontinental geodynamic setting followed by crystal fractionation to generate acid and basic melts. Geochemical and isotopic similarities between the Triassic basic rocks and the Lower Jurassic gabbros from the Limarí Complex in the Coastal Range in central Chile are interpreted as a consequence of a cogenetic event, related to the Mesozoic evolution of this portion of the Gondwana pacific margin.

Key words: Geochemistry, Petrogenesis, Crustal contamination, Triassic volcanism, Coastal Range, central Chile.

RESUMEN

Aporte cortical en la génesis del volcanismo bimodal Triásico de la Cordillera de la Costa, Chile central. El volcanismo Triásico en la Cordillera de la Costa de Chile central está representado por la Formación Pichidangui (31°54'-32°15'S), constituida por flujos de lavas ácidas y básicas con intercalaciones de cuerpos subvolcánicos y rocas sedimentarias. Ambos tipos de lavas presentan un metamorfismo no deformativo de muy bajo a bajo grado. Las características geoquímicas de estas lavas corresponden a las de la serie toleítica, con valores de Nb/Y entre 0,20 y 0,17. Los bajos valores de [mg] en las rocas básicas son indicativos de líquidos no primarios. Las diferencias observadas en elementos traza inmóviles y tierras raras (LREE/HREE, Eu/Eu*) entre las rocas ácidas y básicas son consistentes con sus signaturas isotópicas, cuyos valores iniciales son: $(^{87}Sr/^{86}Sr)_o$ 0,70397-0,70597 y $(^{143}Nd/^{144}Nd)_o$ 0,512515-0,512608 para las rocas básicas y 0,70514-0,71161 a 0,512108-0,512526 en las ácidas. Estas diferencias geoquímicas e

isotópicas entre ambos tipos de lavas se interpretan como consecuencia de diferentes tasas de contaminación cortical a partir de una fuente mantélica enriquecida, con un componente litosférico, en un ambiente extensional intracontinental, seguido por cristalización fraccionada para generar los líquidos ácidos y básicos. Las similitudes geoquímicas e isotópicas observadas entre las rocas básicas del Triásico y los gabros del Jurásico Inferior del Complejo Limarí de la Cordillera de la Costa de Chile central se interpretan como la consecuencia de una génesis común para ambos magmatismos, que estaría relacionada con la evolución mesozoica del margen pacífico de Gondwana.

Palabras claves: Geoquímica, Petrogénesis, Contaminación cortical, Volcanismo Triásico, Cordillera de la Costa, Chile central.

INTRODUCTION

The Coastal Range in central Chile, located between the Pacific Ocean and the Central Valley, is mainly composed of Mesozoic-Cenozoic igneous and sedimentary rocks deposited on a pre-Mesozoic crystalline basement. Exposures of the Triassic rock units in central Chile are poor and scattered (Charrier, 1979; Aguirre, 1985) and for this reason, a new study on these rocks would help to the understanding of the geotectonic and petrological evolution of the Chilean Pacific margin during the beginning of the Mesozoic. These Triassic units correspond to El Quereo, Pichidangui and Los Molles Formations from which only the Pichidangui Formation contains significant volumes of volcanic and subvolcanic rocks.

Previous works concerning the Triassic rocks in the Coastal Range of central Chile are mainly focused on stratigraphic considerations (see, among others, Vicente, 1976; Charrier, 1979 and Rivano and Sepúlveda, 1991, and references therein) or to the plutonic rocks (Gana, 1991; Parada *et al.*, 1991, 1999). Major element data were presented in Vicente (1976), and additional geochemical (major and trace elements) data for the Triassic volcanic rocks are found in Levi *et al.* (1988), Vergara *et al.* (1991) and Cancino (1992).

The results and conclusions of a study on the geochemistry of volcanic rocks from the Pichidangui Formation (31°54'-32°15'S) are reported in this paper. A bimodal (acid and basic) magmatism has already been described for this unit (Vicente, 1976; Vergara *et al.*, 1991; Cancino, 1992). The aim of the present work is to propose a new petrogenetic model for this bimodal magmatism on the basis of their trace element geochemistry, including isotopic (Rb-Sr and Sm-Nd) data. The characterization of this bimodal magmatism, as well as its petrogenetic implications, will be outlined. With this paper, the authors contribute to the understanding of the magmatic evolution of the central Chilean Pacific margin during the beginning of the Mesozoic.

GEOLOGICAL CONTEXT

The Pichidangui Formation (Fig. 1), a 4,000 to 5,000 m thick isoclinal sequence, dipping 15 to 25° to the east-southeast, was deposited in a subaquatic environment. Marine sedimentary rocks predominate in its lower section whereas rocks characteristic of paralic conditions of sedimentation are found at the top where temporary continental conditions are reported (Muñoz Cristi, 1942, 1973; Cecioni and Westerman, 1968; Vicente, 1976; Charrier, 1979; Vergara *et al.*, 1991). Acid and basic lava flows, with intercalations of shales containing a Middle to Late Triassic marine fauna, are typically represented in the Pichidangui Formation; some basic dykes and sills intrude this unit (Vicente, 1976, for a more detailed geographical and stratigraphical information). Basic lavas are mostly restricted to the bottom of this formation, alternating with the acid lavas, the volume of volcanic rocks (mostly acid lavas) decreasing upward, where turbiditic sedimentary rocks and shales with a Late Triassic to Early Jurassic (Hettangian) fauna become predominant. This upper part of the Pichidangui Formation has been assigned by Fuenzalida (1938) and Cecioni and Westermann (1968) to a separate

formation (Los Molles Formation). The Pichidangui Formation overlies conformably the marine El Quereo Formation (graywackes and shales) of Middle Triassic age (Cecioni and Westermann, 1986) which, in turn, rests unconformably on the Arrayán Formation (Fig. 1), a strongly folded rhythmic sequence of slates and sandstones with a Devonian-Late Carboniferous flora (Rivano and Sepúlveda, 1991).

The main interpretative studies of the Pichidangui Formation (see Vergara *et al.*, 1991) are those of Vicente (1976), Charrier (1979), Forsythe *et al.* (1987) and Mpodozis *et al.* (1988). Vicente (1976) considered it as part of a 'Western Euliminar Series' of the 'Andean Orogenic Cycle'. Charrier (1979) invoked deposition in a Triassic graben, probably caused by shearing between the Gondwana continent and a continental or oceanic block located to

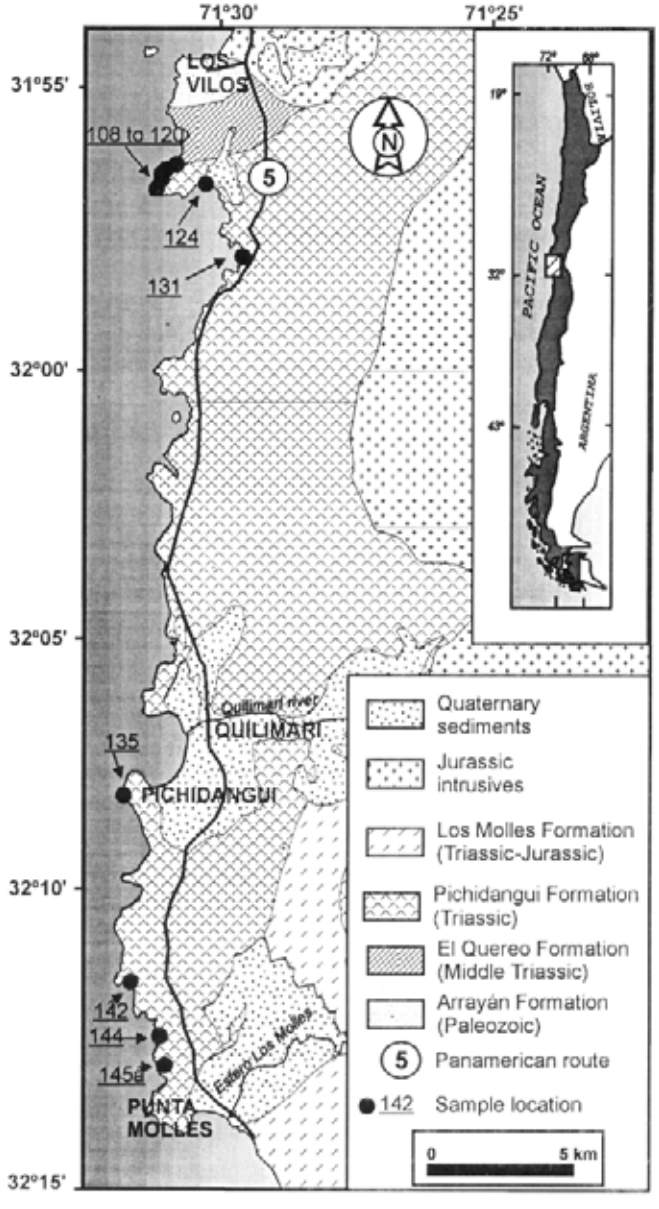

FIG. 1. Geological map of the studied area showing the Triassic and Paleozoic formations in the Coastal Range of central Chile (modified from Arancibia, unpublished map, and Rivano and Sepúlveda, 1991), with location of the studied samples.

the west. On the basis of paleomagnetic data, Forsythe *et al.* (1987) concluded that the coastal Triassic rocks of central-northern Chile (including the Pichidangui Formation) could represent an allochthonous terrane accreted during the Middle to Late Jurassic. Mpodozis *et al.* (1992) included all the upper Paleozoic-Triassic magmatic rocks of central-northern Chile in a Pacific margin magmatic belt of Gondwanaland. Finally, Vergara *et al.* (1991), using major element discriminating diagrams and chondrite normalized rare earth element patterns, interpreted the volcanic rocks of the Pichidangui Formation as: **i-** belonging to a volcanic arc floored by a quasioceanic crust, compatible with an origin at the rim of Gondwanaland before its disintegration; **ii-** a continental/oceanic block located to the west as in Charrier (1979); or **iii-** an allochthonous terrane formed south of its present position as proposed by Forsythe *et al.* (1987).

PETROLOGY

The bimodal character of the Pichidangui Formation was first described by Muñoz-Cristi (1942, 1973) who used the terms keratophyre and quartz-keratophyre to name the silica-rich rocks (lavas, ignimbrite-like breccias and dykes) and the terms oligoclase-augite and labradorite-amphibole diabase for the basic components (lavas, sills and dykes). Cecioni and Westermann (1968) referred to these rocks as keratophyres and andesites, respectively; whereas Vicente (1976) named them keratophyres (albitophyres), spilites and dolerites.

About fifty samples were collected from outcrops of Triassic rocks belonging to the Pichidangui Formation along the Coastal Range between Los Vilos and Punta Molles (Fig.1). According to their field relationships and petrographic characteristics these rocks classify as lithic breccias, lapilli tuffs, ash tuffs, rhyolitic flows with porphyritic seriate textures, basalts, porphyritic basalts, pillow-breccias and related doleritic sills and dykes. In the silica-rich types, quartz, albite and minor K-feldspar appear as phenocrysts in a spherulitic to microcrystalline groundmass. The basic rocks have inequigranular to seriate textures with albitized calcic plagioclase[1] ($An_{21}Ab_{77}Or_2$ to An_1Ab_{99}) and clinopyroxene[1] ($Wo_{36}En_{49}Fs_{15}$ to $Wo_{38}En_{42}Fs_{20}$) as the main phenocrysts. Titanomagnetite, biotite, hornblende and scarce modal quartz (as microcrysts or intergrown with Na-plagioclase and K-feldspar) are the accessory phases. The field relationships, showing an alternation between acid and basic rocks, suggest that they are coeval.

Both, acid and basic rocks, have been affected by non deformational very low- to low-grade metamorphism, giving a prehnite-pumpellyite-epidote association which has been interpreted by Oyarzún *et al.* (1997) as indicative of the transition between the pumpellyite-actinolite, the prehnite-actinolite and the greenschist metamorphic facies.

GEOCHEMISTRY

ANALYTICAL METHODS

Thirteen of the less altered rocks (five basic and eight acid rocks) with loss on ignition values (LOI) under 3% were selected (Table 1). Major and some trace element analyses were performed at the Departamento de Geología (J.M. Martínez, analyst), Universidad de Chile using a Perkin-Elmer P-430 inductively coupled plasma atomic emission spectrometer (ICP-AES). The elements Rb, Nb, Pb, Ta, Hf, U, Tb and Tm were also analyzed in eight of the same samples (110, 111, 113, 114, 118, 120, 124 and 142, see Table 1) at the Centro de Instrumentación Científica, Universidad de Granada, Spain using a Perkin-Elmer Sciex Elan-5000 inductively coupled plasma mass-spectrometer (ICP-MS). The results of the Hf, Th (and Nb only in the acid rocks) ICP-MS analyses for these eight rocks were similar

[1] Electron microprobe analysis (CAMECA SX-50, 20n A, 20 Kv, 3 µ, Universidad de Granada, España).

TABLE 1. SELECTED CHEMICAL ANALYSES OF THE TRIASSIC VOLCANIC ROCKS FROM THE PICHIDANGUI FORMATION (COASTAL RANGE, CENTRAL CHILE). MAJOR ELEMENTS IN WEIGHT PERCENT AND TRACE AND RARE EARTH ELEMENTS IN ppm.

	Basic volcanic rocks					Acid volcanic rocks (lava flows)							
SAMPLE	**111**	**124**	**114**	**108**	**118**	**144**	**113**	**135**	**145a**	**142**	**120**	**131**	**110**
SiO_2	49.20	50.30	51.10	51.30	52.20	69.36	70.00	71.25	71.30	71.62	72.50	76.62	76.70
TiO_2	3.24	2.66	2.65	2.00	1.65	0.50	0.40	0.39	0.35	0.26	0.50	0.25	0.15
Al_2O_3	13.83	15.18	14.50	14.84	15.52	14.20	14.38	13.40	14.52	15.19	13.22	11.20	11.55
Fe_2O_3	1.14	2.84	2.04	1.93	1.32	1.61	0.45	0.46	0.49	0.04	1.31	0.75	0.22
FeO	11.24	8.88	9.60	8.32	8.24	3.64	3.40	3.92	3.36	2.16	3.20	3.20	2.48
MnO	0.21	0.18	0.19	0.17	0.17	0.10	0.06	0.12	0.06	0.03	0.06	0.06	0.04
MgO	4.51	4.40	4.17	5.18	5.28	0.46	0.67	2.07	0.46	0.54	0.40	0.61	0.07
CaO	7.62	7.44	7.43	8.25	7.30	0.60	1.68	0.13	0.04	0.04	0.22	0.47	0.69
Na_20	4.44	4.03	4.25	3.94	4.18	6.27	4.78	5.85	6.13	5.92	6.71	4.49	4.18
K_20	0.62	1.17	0.87	0.86	0.85	1.94	3.06	0.41	2.07	3.32	0.06	1.48	2.80
P_2O_5	0.73	0.25	0.40	0.26	0.36	0.13	0.05	0.09	0.05	0.01	0.11	0.03	0.01
LOI	3.00	2.57	2.76	2.62	2.84	0.99	0.87	2.01	1.09	0.69	1.49	0.95	0.85
Total	**99.78**	**99.90**	**99.96**	**99.67**	**99.91**	**99.80**	**99.80**	**100.10**	**99.92**	**99.82**	**99.78**	**100.11**	**99.74**
[mg]	*0.42*	*0.47*	*0.44*	*0.53*	*0.53*	*0.18*	*0.26*	*0.48*	*0.20*	*0 31*	*0.18*	*0.25*	*0.05*
Ba	130	200	190	200	226	330	500	121	310	350	320	350	1000
Rb	18.3	51.3	30.9		29.0		116.9			48.8	0.3		71.6
Th	1.95	1.90	2.25	*2*	2.04	*8*	10.74	*8*	*7*	5.74	1.85	*13*	13.13
Nb	8.36	5.23	6.68		6.36	*14*	11.69	*9*	*11*	14.30	8.23	*17*	13.58
Sr	170	230	243	260	270	85	110	60	50	84	132	75	95
Zr	218	149	200	164	148	830	430	330	760	312	342	580	280
Y	43	33	40	34	37	62	50	101	59	58	42	83	59
Cr	52	17	29	50	107	3	14	11	7	9	3	8	4
V	400	390	326	290	204	15	22	34	12	14	12	12	11
Ni	18	13	9	20	32	<2	7	6	2	5	3	4	3
Co	48	43	42	39	31	<2	2	<2	<2	<2	<2	<2	<2
Sc	38	33	32	37	30	10	7	5	7	4	12	8	4
Pb	1.61	4.55	3.39		2.76		20.43			7.38	2.45		12.93
Cu	61	34	32	35	43	9	26	6	10	5	8	4	7
Zn	114	102	116	93	91	100	64	165	109	42	58	78	48
Ta	0.65	0.34	0.50		0.40		1.09			1.30	0.62		1.02
Hf	4.79	4.15	4.71	*5*	6.92	*14*	10.47	*7*	*15*	9.45	8.00	*12*	6.76
U	0.51	0.53	0.57		0.60		3.05			1.63	0.96		3.46
La	16	10	13	11	13	28	29	46	35	21	24	44	48
Ce	41	25	33	28	33	70	67	116	81	50	58	108	113
Nd	28	18	23	19	24	39	35	60	44	26	32	57	62
Sm	7.77	5.18	6.50	5.48	6.49	8.63	7.53	14.99	9.97	5.76	7.45	12.73	13.94
Eu	2.40	1.70	2.06	1.84	2.06	1.79	1.18	2.30	1.90	0.74	1.60	2.81	1.73
Gd	7.83	5.84	6.69	5.80	6.31	9.02	6.70	14.00	9.73	6.43	7.10	13.58	10.26
Tb	1.44	1.14	1.20		1.15		1.30			0.57	0.38		1.55
Dy	8.16	6.77	7.32	6.76	7.06	11.04	7.76	16.00	11.27	9.00	7.74	15.37	11.39
Ho	1.60	1.35	1.45	1.28	1.48	2.45	1.64	3.21	2.36	2.00	1.60	3.15	2.22
Er	4.10	3.53	4.09	3.69	3.97	7.14	4.87	7.94	6.65	6.18	4.58	8.67	6.00
Tm	0.68	0.63	0.62		0.63		0.82			0.38	0.23		0.83
Yb	3.98	3.46	3.97	3.57	3.95	7.04	4.62	7.86	6.70	6.10	4.53	8.77	5.98
Lu	0.60	0.52	0.62	0.54	0.61	1.08	0.69	1.15	1.04	0.94	0.70	1.33	0.92

LOI = loss on ignition at 950°C. [mg] = $Mg/(Mg+Fe^{2+})$. Sample 108, basic dike. Th, Hf and Nb in italics; ICP-AES data.

to those obtained using the ICP-AES. Sr and Nd isotope data (Table 2) were obtained for the same eight samples (four acid and four basic rocks) at the Centro de Instrumentación Científica, Universidad de Granada, Spain, using a Finnigan MAT 262 thermal ionization mass spectrometer (TIMS) with variable multicollector and RPQ. Normalization value for $^{87}Sr/^{86}Sr$ was $^{88}Sr/^{86}Sr$ = 8.375209 and the reproducibility under successive determinations of the NBS-987 dissolved standard was better than 0.0007% (2 σ). For the Nd determinations, the normalization value for $^{143}Nd/^{144}Nd$ was $^{146}Nd/^{144}Nd$ = 0.7219, with a precision better than 0.0016% (2 σ) calculated under successive measures of the WSE power standard. The reproducibility under successive measures of the La Jolla dissolution standard was better than 0.0014% (2 σ). Initial isotopic ratios were calculated based on assumed Triassic ages of 220 Ma.

RESULTS

The chemical analyses corroborate the bimodality petrographycally described by Vicente (1976) and Vergara *et al.* (1991) for these rocks. The basic rocks plot into the trachybasalt-traquiandesitic basalt and andesitic basalt fields, whereas the acid rocks plot into the rhyolite field (Fig. 2).

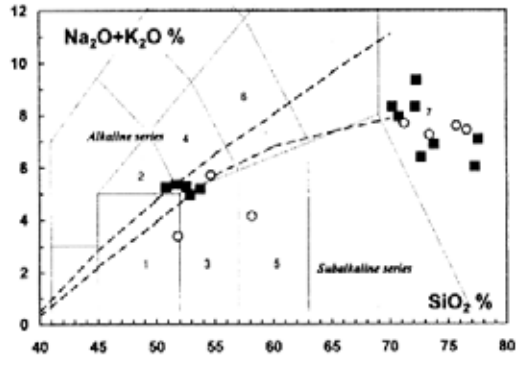

FIG. 2. Total alkali *versus* silica (TAS) diagram for the volcanic rocks of the Triassic Pichidangui Formation, Coastal Range of central Chile. **Full squares**= this paper; **open circles=** data from Vergara *et al.* (1991). **1-** basalt; **2-** trachybasalt; **3-** basaltic andesite; **4-** basaltic trachyandesite; **5-** andesite; **6-** trachyandesite; **7-** rhyolite (after Le Bas *et al.*, 1986). Rocks are plotted as anhydrous analyses. Alkaline *versus* sub-alkaline boundaries (discontinuous lines) are from Rickwood (1989).

Both, acid and basic rocks, plot along the alkaline-subalkaline boundary. The scattering of the alkalis observed in the acid rocks may be a consequence of the known mobility of these elements during low-grade metamorphic processes. Consequently, the discrimination between alkaline and subalkaline affinities becomes obscured due to the alteration phenomena. In this respect, in the SiO_2 *versus* Nb/Y diagram (not shown), the basic rocks plot into the subalkaline basalt and andesite fields, and the acid rocks between those of rhyolite-rhyodacite fields. In this diagram, both types of rocks show similar Nb/Y ratios (mean of 0.20 for the acid rocks and 0.17 for the basic rocks), both indicating a subalkaline affinity. The projection of the clinopyroxene composition into the Leterrier *et al.* (1982) diagrams also indicates a subalkaline affinity for them, plotting along the tholeiitic and calc-alkaline fields boundary.

The Al_2O_3 values range between 13.83 and 15.52% in the basic rocks and 11.20 to 15.19% in the acid rocks. The MgO values are in the interval 4.17-5.28% in the basic rocks, and between 0.07 and 2.07% in the acid rocks (Table 1). The [mg] values (=Mg/(Mg+Fe^{2+})) are in the range 0.52-0.53 in the basic and 0.05-0.48 in the acid rocks with the highest [mg] values in the silica-rich rocks corresponding to the rhyolites. Dispersion in these [mg] values in rhyolites is a consequence of the mobility of Mg (and Fe^{2+}) in this type of rocks during the secondary alteration. CaO in the basic rocks range from 7.30 to 8.25% indicating that, in spite of the albitization of the primary Ca-rich plagioclase, these rocks behaved as a 'closed-system' to the CaO mobility during very-low grade metamorphism. On the contrary, in the acid rocks, the low CaO values (0.04-1.68%) are due to the higher albitic component of the plagioclase phenocrysts. The K_2O contents vary from 0.62 to 1.17% in the basic rocks and from 0.06 to 3.32% in the acid ones. TiO_2 and P_2O_5 are in the ranges 1.65-3.24% and 0.25-0.73%, respectively for the basic rocks and 0.15-0.50% and 0.01-0.13%, respectively, for the acid rocks. The last two oxides show a negative correlation with the SiO_2 content. The Al_2O_3 content of the basic rocks as well as the projection of both, basic and acid rocks, on the FeO/MgO *versus* SiO_2 diagram (Fig. 3) and the AFM and Jensen (1976, *in* Rollinson, 1993, not shown) diagrams suggest a tholeiitic rather than a calc-alkaline affinity for these Triassic rocks.

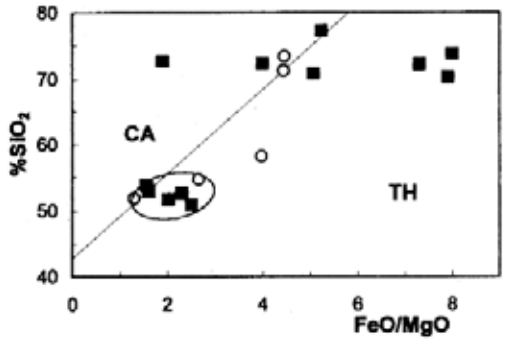

FIG. 3. FeO/MgO *versus* SiO_2 diagram for the volcanic rocks of the Triassic Pichidangui Formation, Coastal Range of central Chile. Boundary between the tholeiitic (TH) and calc-alkaline (CA) is taken from Miyashiro (1971). Symbols as in figure 2. Basic rocks are circled.

Differences between acid and basic rocks are also reflected in their trace element contents. Major differences between these two types of rocks can be observed in a N-MORB normalized spidergram. In the basic rocks (Fig. 4a) almost all incompatible elements have normalized values between 1 to 10 times the N-MORB and the overall pattern shows an enrichment in K_2O, Rb, Ba and Th (with Rb•Th) and a decrease in enrichment from Ta to Y, with a characteristic Ta-Nb trough. Normalized values for Yb and Sc are close to N-MORB, whereas Cr is depleted with respect to it. In the acid rocks (Fig. 4b), the N-MORB normalized spidergrams have, in general, similar patterns characterized by a strong enrichment (> 10 times) in K_2O, Rb, Ba and Th

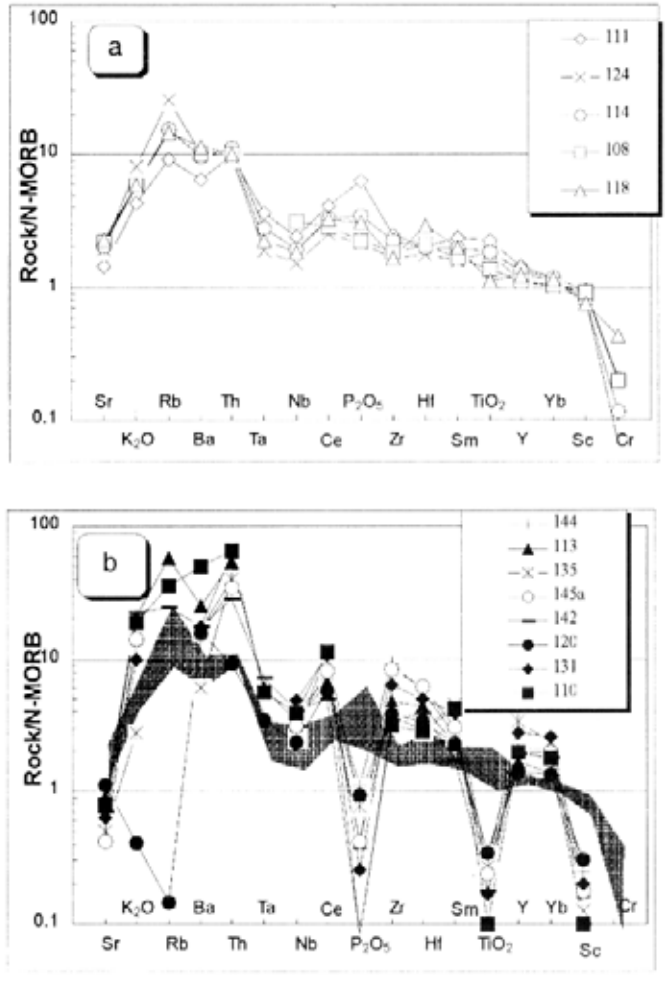

FIG. 4. Trace element spidergrams normalized to N-MORB (Pearce, 1982) for the volcanic rocks of the Triassic Pichidangui Formation, Coastal Range of central Chile; **a-** basic rocks; **b-** acid rocks; shaded area represents the spectrum of the basic rocks.

TABLE 2. Sr-Nd ISOTOPIC DATA FOR THE VOLCANIC ROCKS OF THE PICHIDANGUI FORMATION, COASTAL RANGE OF CENTRAL CHILE.

Sample	Type	Age (Ma)	Rb	Sr	Sm	Nd	$^{87}Sr/^{86}Sr$	$^{143}Nd/^{144}Nd$	$(^{87}Sr/^{86}Sr)_0$	$(^{143}Nd/^{144}Nd)_0$	εNd^t_{CHUR}	t_{DM} (Ga)
111	β	220	18.3	170	7.77	28	0.706949	0.512787	0.70597	0.512545	3.72	0.92
124	β	220	51.3	230	5.18	18	0.705979	0.512859	0.70396	0.512608	4.95	0.81
114	β	220	30.9	243	6.50	23	0.705705	0.512761	0.70455	0.512515	3.12	1.05
118	β	220	29.0	270	6.49	24	0.706231	0.512780	0.70526	0.512544	3.70	0.87
113	ρ	220	116.9	110	7.53	35	0.714758	0.512670	0.70514	0.512483	2.50	0.74
142	ρ	220	48.8	84	5.76	26	0.714721	0.512719	0.70946	0.512526	3.34	0.69
120	ρ	220	0.3	132	7.45	32	0.707512	0.512640	0.70749	0.512437	1.61	0.89
110	ρ	220	71.6	95	13.94	62	0.718434	0.512304	0.71161	0.512108	-4.81	1.43

β: basalt; ρ: rhyolite. $^{87}Rb/^{86}Sr$ and $^{147}Sm/^{144}Nd$ were calculated from the elemental concentrations of Rb, Sr, Sm and with the following ratios: $^{87}Rb/^{86}Sr = 2.8925 \times Rb/Sr$ and $^{147}Sm/^{144}Nd = 0.6049 \times Sm/Nd$ (Vidal, 1994). Concentrations of Rb, Sr, Sm, and Nd are in ppm. Model Nd ages are calculated with reference to the depleted mantle reservoir.

(Rb▲ Th). With the exception of Sr, P_2O_5, TiO_2 and Sc, the rest of the trace elements are also enriched with respect to the N-MORB (1 to 10 times). The strong negative anomalies shown by P_2O_5 and TiO_2 and the depletion in Sc and Cr (values for this last element plot below the 0.1 line in Fig. 4b) are typical features in these acid rocks which also show a negative Ta-Nb anomaly. The scattering in the K_2O, Rb and Ba values (Fig. 4b) are mainly related to the mobility of these elements during low-grade metamorphism. With the exception of the strong P_2O_5 and TiO_2 anomalies in the acid rocks, the spidergrams of these and those of the basic types tend to be rather similar, with higher values for the acid rocks.

The chondrite-normalized diagrams for the rare earth elements (REE) show similarities and differences between the basic and acid types (Figs. 5a and 5b). The basic rocks (Fig. 5a) have a rather flat pattern, with 30-50 times the chondrite values for the light rare earth elements (LREE) and about 20 times that value for the heavy rare earth elements (HREE). No significant Eu anomaly is present in these basic rocks, which are characterized by average $(La/Lu)_N$, $(La/Sm)_N$ and $(La/Ce)_N$ ratios of 2.2, 1.2 and 1.0, respectively. The acid rocks (Fig. 5b) have higher total REE values, 60 to 140 times the chondritic values for the LREE and 20 to 45 times for the HREE. A conspicuous negative Eu anomaly is present in these rocks ($Eu/Eu^* = 0.51$) and their average $(La/Lu)_N$, $(La/Sm)_N$ and $(La/Ce)_N$ ratios are 3.7, 2.3 and 1.1, respectively, showing rather parallel patterns with respect to those of the basic lavas.

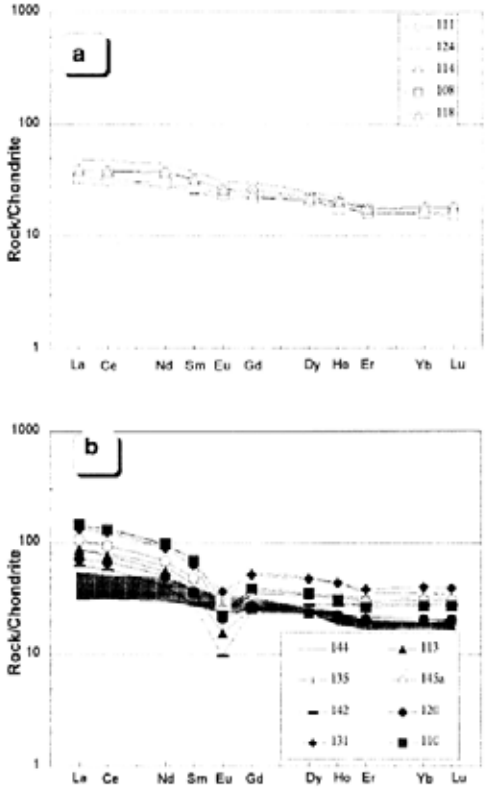

FIG. 5. Rare earth element diagrams normalized to chondrite (Nakamura, 1974) for the volcanic rocks of the Triassic Pichidangui Formation, Coastal Range of central Chile. **a**- basic rocks; **b**- acid rocks; shaded area represents the spectrum of the basic rocks.

Initial isotopic data (Table 2) confirm the existence of a difference between the basic and acid rocks. The $(^{87}Sr/^{86}Sr)_o$ values for the former are in the range 0.70397-0.70597, whereas in the latter a wider interval (0.70514-0.71161) exists. Concerning the $(^{143}Nd/^{144}Nd)_o$ ratio, smaller differences are found between the two types of rocks, with values ranging from 0.512515-0.512608 in the basic rocks and from 0.512108-0.512526 in the acid types. Initial $^{87}Sr/^{86}Sr$ ratios (about 0.7034) have been reported for a basic lava flow from the Pichidangui Formation (Nystrõm, unpublished information, *in* Vergara *et al.*, 1995). Among the acid rocks, the highest $(^{87}Sr/^{86}Sr)_o$ and lowest $(^{143}Nd/^{144}Nd)_o$ values correspond to the rhyolite (sample 110) with the highest SiO_2 content (76.70%) which is the only specimen with a negative value of $\varepsilon Nd^{t}_{CHUR}$ (-4.81, Table 2).

PETROGENESIS

The relatively moderate alteration of the rocks selected for chemical analysis (reflected in the restricted dispersion of the immobile trace elements) means that they are close representatives of their original chemical compositions. Bimodal magmatism, without significant volumes of magma with an intermediate composition, is common in many anorogenic continental extensional settings (*e.g.*, Doe *et al.*, 1982; Garland *et al.*, 1995) and in continental margins of back-arc extensional basin environments (McCulloch *et al.*, 1994; Gibbons and Young, 1999). In the Upper Triassic-Lower Jurassic plutonic complexes of the Coastal Range in central Chile, a bimodal magmatism also exists with the presence of related leucogranites and gabbros. A crustal component has been proposed for the genesis of the leucogranites (Gana, 1991; Parada *et al.*, 1991, 1999), whereas, for the genesis of the Mesozoic gabbros, an asthenospheric dominated source is invoked (Parada *et al.*, 1999). According to Huppert and Sparks (1988), crustal melting by intrusion of basaltic magmas could permit the generation of silicic magmas and, consequently, the development of a bimodal suite like the one which characterizes the Triassic volcanism in the Coastal Range of central Chile. In order to explain the petrogenesis of this bimodal magmatism, two main aspects must be investigated: one concerns the nature of the basic magma source and the other refers to the genesis of the related acid rocks and the probable crustal participation in their composition. Three different questions can be proposed: **1-** are both basic and acid contaminated magmas derived from different mantle source?; **2-** are both cogenetic magmas only related by fractionation?; and **3-** are both cogenetic magmas with different crustal contamination degrees?

A major restriction in the characterization of the basic magma source in this case is the absence of primitive mantle-derived liquids as indicated by the low [mg], Cr and Ni values in the analyzed basic rocks, which suggest olivine (and/or clinopyroxene?) fractionation. Nevertheless, trace element ratios, together with isotopic values, can help to obtain some information regarding the genesis of this basic magma.

Concerning the variations of trace elements and specially the REE (Figs. 4 and 5), the almost parallel patterns of acid and basic rocks could be interpreted as due to a genetic link between these two rock types. In fact, the acid rocks could derive from the basic ones by fractionation of clinopyroxene, Ca-rich plagioclase, Ti-magnetite and apatite as suggested by the depletion in Sc, V, Cr (elements compatible with clinopyroxene), TiO_2 and P_2O_5 and the strong negative Eu anomaly shown by the acid rocks. In fact, simple mass balance calculations point to a probable evolution from the basaltic melts to the acid liquids by a fractionation of 30% clinopyroxene, 20% plagioclase, 10% Ti-magnetite and ♠ 1% apatite. However, the gap and differences which exist in the isotopic initial ratios (Table 2) between acid and basic rocks must be interpreted on the light of another petrogenetic process such as crustal contamination.

Geochemical evidence of crustal contamination in the genesis of these Triassic rocks is the enrichment in elements from the crust such as K, Ba, Rb, Th and LREE and the decrease in Ta and Nb. The trace element patterns normalized to N-MORB show enrichment in K, Rb, Ba and Th and a slight negative Ta anomaly, which is more marked in the acid rocks (Figs. 4a and b). Crustal components are, therefore, more evident in the acid rocks. Ratios of trace

elements with similar incompatibilities are different for the basic and acid rock types (*e.g.*, mean values in basic *versus* acid rocks of La/Nb = 1.95 *versus* 2.91; Zr/Nb = 26.9 *versus* 40.0; Ti/V = 47.0 *versus* 141.8; La/Yb = 3.3 *versus* 5.4; Zr/Yb = 46.3 *versus* 75.7). Moreover, the characteristically low TiO_2 and P_2O_5 contents in the rhyolites with respect to N-MORB (Fig. 4b) can also point to a crustal component in their genesis considering the low values of these two elements in the upper crustal rocks (*e.g.*, Wedepohl, 1995).

In the geotectonic discrimination diagram by Cabanis and Lecolle (1989), the basic rocks plot in the intracontinental and post-orogenic domain corresponding to the field of basalts generated in a back-arc basin context (Fig. 6a). Projection of the chemistry of these same basic rocks in other geotectonic discriminant diagrams (*e.g.*, the Zr/4:2Nb:Y diagram of Meschede, 1986, Ti/100:Zr:Y*3, Pearce and Cann, 1973, not shown here) confirm the within plate extensional character of these rocks. In the Nb *versus* Y diagram by Pearce *et al.* (1984), the acid rocks plot mainly in the within-plate field close to the triple joint (Fig 6b), whereas according to the Eby (1992) diagrams for granitic rocks, these rocks plot in the A_2-type, which correspond to acid rocks generated in the region of continental margin and island-arc basalts. The projection of both types of rocks in the same 'within-plate extensional field' setting is consistent with the presence of a geodynamic extensional regime in the Coastal Range of central Chile (Charrier, 1979) during the genesis of these Triassic rocks.

With respect to the source of this magmatism, values of the ratio La/Nb > 1.5 in basaltic rocks have been interpreted as indicative of a lithospheric component in the genesis of these magmas (Thompson and Morrison, 1988). In this sense, the enrichment in high field strength elements (Nb to Yb in Fig. 4a) with respect to the N-MORB in the basic rocks is indicative of a mantle source more enriched than N-MORB. Also, the marked Ta-Nb trough (Fig. 4a, b) is indicative of a crustal (subduction-related?) component in their genesis. The rocks from the Pichidangui Formation have been also represented in the Ta/Yb *versus* Th/Yb diagram (Fig. 7). In this diagram, normalization of Th and Ta with respect to Yb minimizes the effect of partial melting as well as effects related to the fractional crystallization (Pearce, 1982). Due to the enrichment of Th with

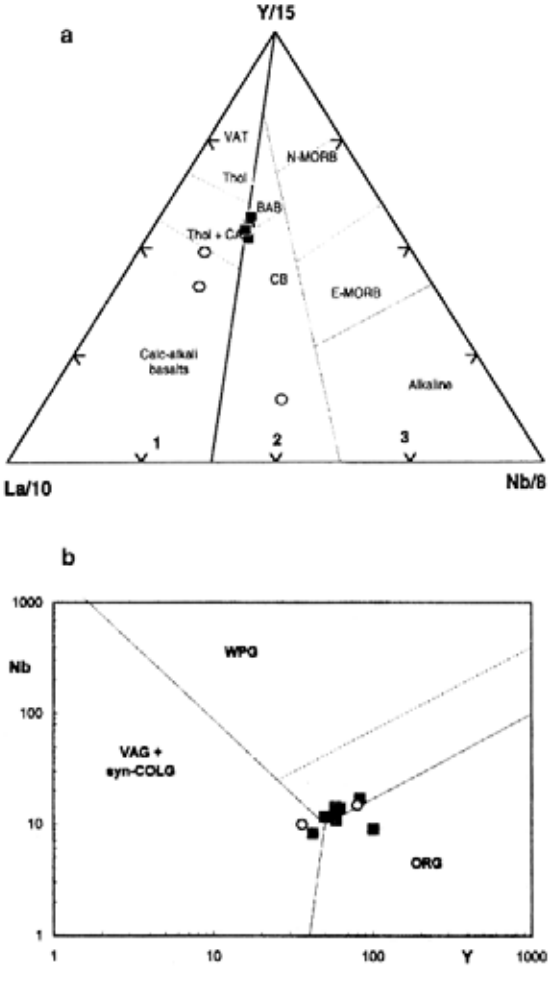

FIG. 6. Tectonic discrimination diagrams for the volcanic rocks of the Triassic Pichidangui Formation, Coastal Range of central Chile. **a-** basic rocks plot in the Cabanis and Lecolle (1989) diagram; **1-** orogenic domains; **2-** intracontinental and post-orogenic domains; **3-** anorogenic domains. **CA-** calc-alkaline basalts; **VAT-** volcanic arc tholeiites; **CB-** continental tholeiites; **BAB-** basalts generated in fore- and back-arc basins; **E-MORB-** enriched mid-ocean ridge basalts; **N-MORB-** normal mid-ocean ridge basalts. Symbols as in figure 2. **b-** Nb *versus* Y discrimination diagram for acid rocks (after Pearce *et al.*, 1984). **WPG**-within plate granites; **ORG-** orogenic granites; **VAG-** volcanic arc granites; **syn-COLG-** syn-collisional granites. The broken line is the field boundary for ORG from anomalous ridges. Symbols as in figure 2.

respect to Ta in the continental crust, processes related to crustal contamination would be represented by compositional trends along the *C* vector and those related with a subduction component along the *S* vector in figure 7. In this case, both types of rocks plot out of the within-plate (*W*) or fractional (*f*) trends proposed by Pearce (1982, 1983) and are mainly aligned following the crustal-subduction *C-S* vectors. The authors interpret this trend as a consequence of an increase in the Th content in the basic and acid rocks, probably due to crustal contamination from an enriched mantle source. Crustal contamination would also explain the fact that both, basic and acid rocks, plot in the calc-alkaline field in the 'active continental margins' of figure 7.

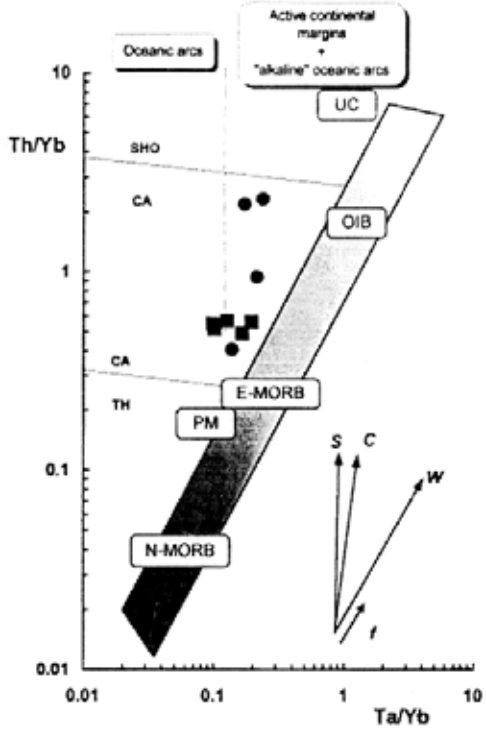

FIG. 7. Ta/Yb *versus* Th/Yb diagram (after Pearce, 1982, 1983) for the volcanic rocks of the Triassic Pichidangui Formation, Coastal Range of central Chile. **C-** vector of the crustal contamination trend; **W-** within-plate enrichment vector; **S-** subduction-zone enrichment vector; **f-** fractional crystallization vector. **SHO-** shoshonitic series; **CA-** calc-alkaline series; **TH-** tholeiitic series. Mid-ocean ridge and within plate volcanic rocks plot along the diagonal shaded band. **Full squares=** basic rocks; **full circles=** acid rocks. **UC-** average composition of the upper continental crust (after Wedepohl, 1995). Primitive mantle (**PM**), **N-MORB**, **E-MORB** and **OIB** values from Sun and McDonough (1989).

The Sr-Nd isotopic data represented in figure 8 show the basic rocks plotting close or into the mantle array and near to the prevalent mantle reservoir component (PREMA) end member. This mantle reservoir, defined by the values $^{143}Nd/^{144}Nd = 0.5130$ and $^{87}Sr/^{86}Sr = 0.7033$, was proposed by Zindler and Hart (1986) and represents the most common isotopic composition of basalts from oceanic islands, intra-oceanic island arcs and continental basalt suites. E-type MORB (as representative of a enriched mantle source) has isotopic values of $^{143}Nd/^{144}Nd = 0.51299$-$0.51300$ and $^{87}Sr/^{86}Sr = 0.70280$-$0.70334$ (Rollinson, 1993), plotting close to the PREMA end member in figure 8. In the same figure, the acid rocks from the Pichidangui Formation show a high $(^{87}Sr/^{86}Sr)_o$ dispersion, possibly related to the mobility of Sr during very-low grade metamorphism, limiting the applicability of their isotopic petrogenetic implications only to the less altered rocks.

On the light of the isotopic data, positive εNd and Sr isotope ratios around 0.704 for the basic rocks can be interpreted as the consequence of an enriched (lithospheric dominated) component in their source. In this sense, the representation of the Lower Jurassic bimodal plutonism from the Coastal Range of central Chile plotted in figure 8 reveals the isotopic similarities between the gabbros of the Limarí Complex (Rb/Sr radiometric ages from 220 to 200 Ma, *in* Gana, 1991) and the basic rocks of the Pichidangui Formation, both with a εNd value *ca.* 4. Also, both Jurassic gabbroic rocks and the basic lavas of the Pichidangui Formation, have similar model Nd ages (*ca.* 1 Ga, Table 2), which would point out to a similar (or common?) petrogenetic setting. In accordance with the origin proposed by Parada *et al.* (1999) for the Lower Jurassic gabbros, an enriched source component is necessary to explain the isotopic signature of the basic Triassic volcanic rocks of the Pichidangui Formation.

The acid volcanic rocks need a more Sr radiogenic and a lower εNd component for their genesis. Their trace element characteristics point to the influence of a crustal component at their origin. A comparison with the coeval plutonic rocks of the Coastal Range of central Chile may help to find genetic relationships with the Si-rich Triassic lavas. The composition of the Lower Jurassic granites of the Coastal Range of central Chile represented in figure 8 suggests a

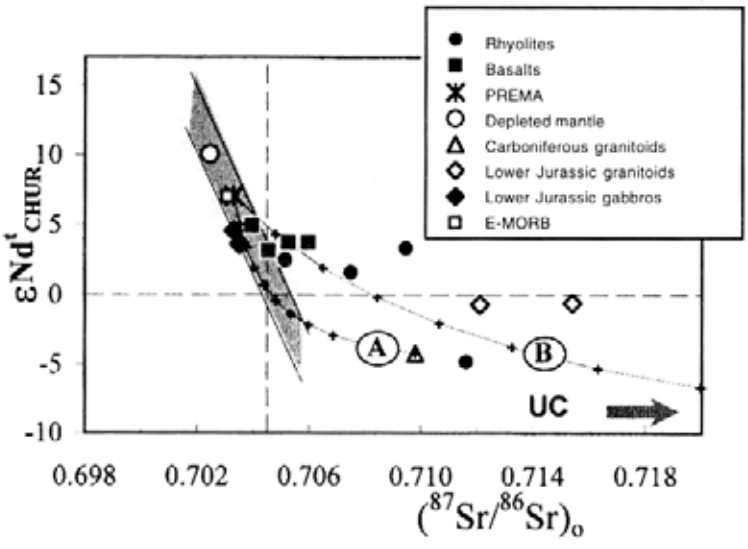

FIG. 8. $(^{87}Sr/^{86}Sr)_o$ *versus* εNd^t_{CHUR} (calculated to 220 Ma) for the volcanic rocks of the Triassic Pichidangui Formation, Coastal Range of central Chile. Symbols as follows: **full squares**= basic rocks; **full circles**= acid rocks; **open triangle** = Carboniferous granitoids (Santo Domingo Complex, sample F2-24 with $^{87}Sr/^{86}Sr = 0.7098$; Sr = 115 ppm; $^{143}Nd/^{144}Nd = 0.512027$; Nd = 35.7 ppm, Parada *et al.*, 1999); **full diamonds** = Lower Jurassic gabbros (Limarí Complex, Parada *et al.*, 1999); **open diamonds** = Lower Jurassic granitoids (Limarí Complex, Parada *et al.*, 1999). Values for the depleted mantle (**DM**), prevalent mantle (**PREMA**) and mantle array (shaded area) taken from Rollinson (1993). **UC=** Upper Continental Crust ($^{87}Sr/^{86}Sr = 0.7369$; Sr = 160 ppm; $^{143}Nd/^{144}Nd = 0.51212$; Nd = 31 ppm) from Faure (1986). **Path A**= mixing model between PREMA and Carboniferous granitoids; **path B**= mixing model between PREMA and UC. Compositional intervals in both paths are indicated by crosses each 10%.

crustal source or a major participation of a crustal component in their genesis. The projection of the more silica-rich granitoids from the Coastal Range Carboniferous Santo Domingo Complex (Parada *et al.*, 1999) allows to estimate the crustal component in the genesis of the Triassic bimodal volcanism of the Pichidangui Formation. A mixing curve is plotted in figure 8 applying the mixing equation in Faure (1986):

$$e^x_M = \frac{e^x_A X_A f + e^x_B X_B (1-f)}{X_A f + X_A (1-f)}$$

where X_A , X_B are the concentrations of the element X and εA^x and εB^x are the relevant isotope parameters of element X in components A and B for values of f ranging from $f = 1$ (pure A) to $f = 0$ (pure B). The PREMA reservoir is taken as the mantle source. For the contaminant, two end members are considered: the Carboniferous granitoids of the Coastal Range (path A) and a representative value of the upper continental crust (path B). In both model paths, the crustal component in the isotopic signature of the basic rocks is around 10%. A higher crustal component must be necessary to obtain the isotopic signature of the acid rocks. The large mobility of Sr during low-grade metamorphic processes must be also responsible for the relatively high dispersion in the Sr isotopic data which complicates the determination of the amount of crustal component.

With the aim to minimize the influence of Sr mobility, a similar mixing curve has been designed using the Th content (Fig. 9). In this case, the equation for the mixing curve is a simple mass balance:

$$C_M = C_A f + C_B (1-f)$$

in which C_M is the concentration of the element i in the mixing between the components A and B for values of f ranging from $f = 1$ (pure A) to f = 0 (pure B). As in figure 8, mixing curves were constructed using the Carboniferous granitoids (path A) and the upper continental crust (path B) as contaminants, whereas the E-type MORB was chosen as an enriched mantle reservoir. In this case, similar conclusions can be obtained with respect to figure 8. A low crustal component is observed in the

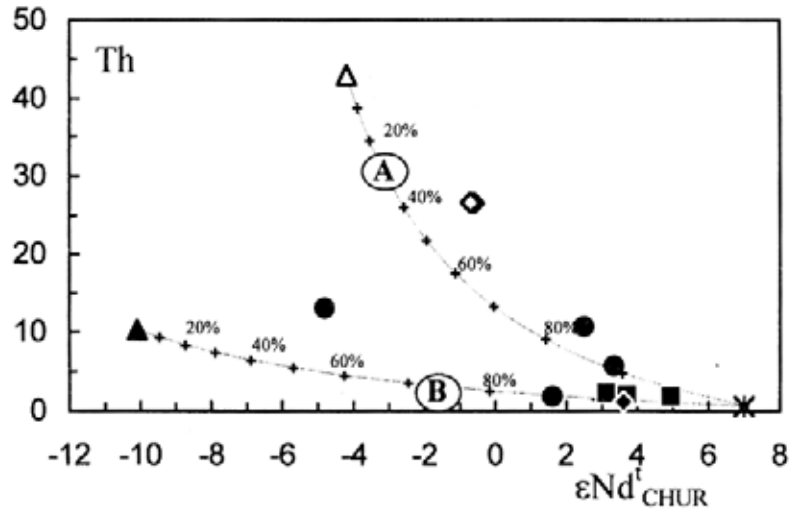

FIG. 9. $\varepsilon Nd^{t}_{CHUR}$ (calculated to 220 Ma) *versus* Th (in ppm) diagram for the volcanic rocks of the Triassic Pichidangui Formation, Coastal Range of central Chile. Symbols and source of the geochemical data as in figure 8 except for ✱ = E-MORB; UC and E-MORB Th values (=10.3 and 0.60 ppm respectively) are taken from Wedepohl (1995) and Sun and McDonough (1988), respectively. **Path A=** mixing model between E-MORB and Carboniferous granitoids. **Path B=** mixing model between E-MORB and UC. Compositional intervals in both paths are marked by crosses and numbers indicating the participation of mantelic component in the mixing.

genesis of the basic Triassic lavas (as well as for the Lower Jurassic gabbros of the Limarí Complex) whereas a higher crustal component (around 20%) is needed to generate the acid rocks. Sample 110, with $\varepsilon Nd^{t}_{CHUR}$ = -4.81 plots out of the mixing curves between the mantle reservoir and the Carboniferous granitoids. This rhyolite is the most acid of the studied rocks and its origin must be related to a maximum of crustal melting, as can be interpreted on the light of its isotopic and trace element geochemistry.

CONCLUSIONS

According to the new trace element and isotopic data presented, the Triassic volcanism of the Pichidangui Formation is characterized by a tholeiitic bimodal suite. The basic magmas, with La/Nb > 1.5, $(^{87}Sr/^{86}Sr)_{o}$ in the range 0.70396-0.70597, and $\varepsilon Nd^{t}_{CHUR}$ 34, would be related to an enriched lithospheric dominated source. A weak contamination by a crustal component is apparent in the genesis of these basic lavas. The acid rocks show geochemical evidences of a larger crustal component at their origin (Figs. 4b, 7, 8 and 9). The projection of different elements characterizing the geochemistry of this Triassic magmatism into various discriminant tectonomagmatic diagrams, indicates a continental extensional setting for the genesis of the magmatism, corroborating the extensional geotectonic model proposed by Charrier (1979) and Mpodozis and Kay (1992) for the Triassic pacific Gondwana margin.

Isotopic geochemical similarities between the basic rocks of the Pichidangui Formation and the geographically close Lower Jurassic (220 to 200 Ma, *in* Gana, 1991) gabbros of the Limarí Complex (Figs. 8 and 9) have been established here. Their similar $(^{87}Sr/^{86}Sr)_{o}$, model t_{DM} ages and $\varepsilon Nd^{t}_{CHUR}$ values, could be interpreted in terms of a common enriched mantle source for both types of basic rocks. The following, simplified petrogenetic model (Fig. 10) is proposed to explain this magmatism. During Late Triassic to Early Jurassic times, an extensional geotectonic setting developed in the pacific Gondwana margin, accompanied by an upwelling of enriched mantle material. Melting of

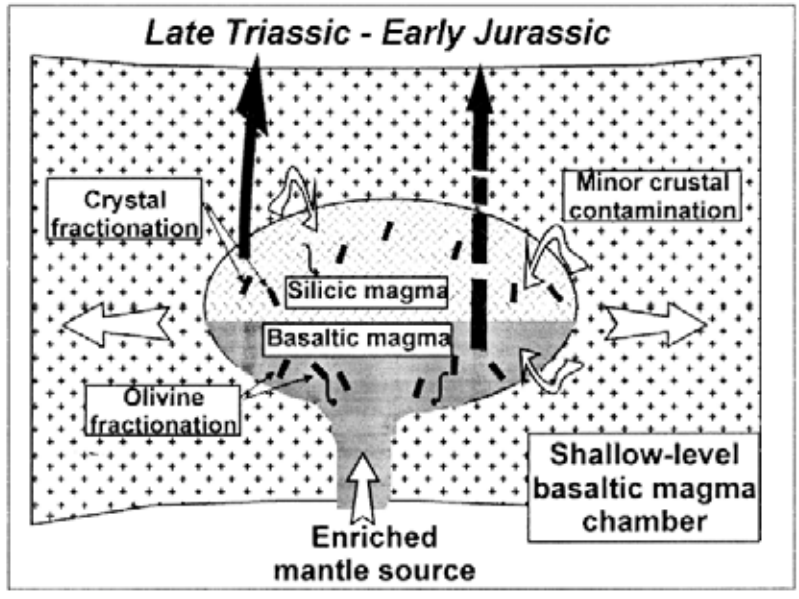

FIG. 10. Schematic model of a two-stage shallow-level basaltic magma chamber in an extensional geotectonic setting during the Late Triassic-Early Jurassic in central Chile. The intrusion of basaltic melts into continental crust would permit the segregation of two liquids with different viscosity. The interaction between the basaltic (enriched mantle source) liquids and the pre-Triassic continental crust is reflected by minor continental contamination in the basaltic magma and slightly higher in the silicic magma originated by higher crustal melting. Later crystal fractionation in each of the two generated liquids would be responsible for the Triassic bimodal magmatism in the Pichidangui Formation.

this enriched (lithospheric dominated) mantle would generate an enriched basaltic liquid which was emplaced in a shallow level magma chamber. Contamination by the continental crust (dominated by Carboniferous granitoids) would occur in this shallow magma chamber, with higher assimilation degrees of crustal material, derived from partial melting of the roof rocks, in the upper zone. According to this model two liquids, with different viscosity and slightly different initial isotopic signatures, would be generated, resulting in a less dense, chemically isolated upper level, and a higher density, basaltic liquid in the lower level of this shallow magma chamber. These two levels of the chamber would evolve in a chemically independent way. Olivine fractionation took place in the lower level, originating the evolved basaltic liquids of the Pichidangui Formation, whereas a *ca.* 67% closed fractionation occurred in the upper level giving rise to the rhyolitic liquids, with slightly contrasted isotopic signatures with respect to those of the lower basaltic level. The final emplacement of these two differentiated liquids would have originated the bimodal magmatic pattern of the Pichidangui Formation. A similar two-stage petrogenetic model has been proposed by McCulloch *et al.* (1994) for the genesis of the bimodal (basalts and rhyolites) back-arc basin volcanism in the Taupo Volcanic Zone of New Zealand. The petrogenetic model proposed here explains why the silicic rocks, with isotopic compositions not significantly different from those of the associated basalts, cannot be interpreted as the result of pure melting of the crustal basement (*e.g.*, Carboniferous granitoids). On the other hand, deep crystallization in a different (?) basaltic magma chamber would have generated the Lower Jurassic (220-200 Ma) gabbros of the Limarí Complex which, according to the model proposed, would be cogenetic with the bimodal magmatism of the Triassic Pichidangui Formation.

ACKNOWLEDGEMENTS

This work has been supported by the FONDECYT Project 1961108.The authors thank Dr. F. Bea (Universidad de Granada, Spain) for the analytical facilities with the ICP-MS and TIMS analyses. The authors thank P.T Leat (British Antarctic Survey), B. Levi (Stockholm University) and M.A. Parada (Universidad de Chile) for their comments and suggestions which considerably improved the original manuscript. This paper is a contribution to the IGCP Project 436 'Gondwana Pacific Margin'.

REFERENCES

Aguirre, L. 1985. The Southern Andes. *In* The ocean basins and margins, The Pacific Ocean (Nairn, A.E.M.; Stehli, F.G.; Uyeda, S.; editors) . *Plenum Press*, Vol. 7A, p. 265-376. New York.

Cabanis, B.; Lecolle, M. 1989. Le diagramme La/10-Y/15-Nb/8: un outil pour la discrimination des séries volcaniques et la mise en evidence des processus de mélange et/ou de contamination crustales. *Comptes Rendus de l'Académie des Sciences de Paris*, Série 2, Vol. 309, p. 2023-2029.

Cancino, A. 1992. Contribución a la petrología e interpretación tectónica de las rocas volcánicas triásicas y jurásicas de la región central de Chile (32°-34°S). Memoria de Titulo (Inédito), *Universidad de Chile*, 259 p.

Cecioni, G.; Westermann, G. 1968. The Triassic/Jurassic marine transition of coastal central Chile. *Pacific Geology*, Vol. 1, p. 41-75.

Charrier, R. 1979. El Triásico en Chile y regiones adyacentes de Argentina: una reconstrucción paleogeográfica y paleoclimática. *Comunicaciones*, Vol. 26, p. 137.

Doe, B.R.; Leeman, W.P.; Christiansen, R.L.; Hedge, C.E. 1982. Lead and strontium isotopes and related trace elements as genetic tracers in the Upper Cenozoic rhyolite-basalt association of the Yellowstone Plateau volcanic field. *Journal of Geophysical Research*, Vol. 87, B6, p. 4785-4806.

Eby, G.N. 1992. Chemical subdivision of the A- type granitoids: petrogenetic and tectonic implications. *Geology*, Vol. 20, p. 641-644.

Faure, G. 1986. Principles of isotope geology. 2nd edition. *Wiley*, 589 p. New York.

Forsythe, R.D.; Kent, D.V.; Mpodozis, C.; Davidson, J. 1987. Paleomagnetism of Permian and Triassic rocks, central Chilean Andes. *In* Structure, tectonics and geophysics (McKenzie, G.A.; editor). *American Geophysical Union, Geophysical Monograph*, Vol. 40, p. 241-251.

Fuenzalida, V. 1938. Las capas de Los Molles. *Boletín del Museo de Historia Natural*, Vol. 16, p. 6-98. Santiago.

Gana, P. 1991. Magmatismo bimodal del Triásico Superior-Jurásico Inferior, en la Cordillera de la Costa, provincias de Elqui y Limarí, Chile. *Revista Geológica de Chile*, Vol. 18, p. 55-67.

Garland, F.; Hawkesworth, C.J.; Montovani, S.M. 1995. Description and petrogenesis of the Parana rhyolites, Southern Brazil. *Journal of Petrology*, Vol. 36, p. 1193-1227.

Gibbsons, W.; Young, T.P. 1999. Mid-caradoc magmatism in central Lyôn, rhyolite petrogenesis, and evolution of the Snowdonia volcanic corridor in NW Wales. *Journal of the Geological Society of London*, Vol. 156, p. 301-316.

Huppert, H.E.; Sparks, R.S.J. 1988. The generation of granitic magmas by intrusion of basalt into continental crust. *Journal of Petrology*, Vol. 29, p. 599-624.

Le Bas, M.J.; Le Maitre, R.W.; Streckeisen, A.; Zanettin, B. 1986. A chemical classification of volcanic rocks based on the total alkali-silica diagram. *Journal of Petrology*, Vol. 27, p. 745-750.

Leterrier, J.; Maury, R.C.; Thonon, P.; Girad, D.; Marchal, M. 1982. Clinopyroxene composition as a method of identification of the magmatic affinities of paleovolcanic series. *Earth and Planetary Science Letters*, Vol. 59, p. 139-154.

Levi, B.; Nyström, J.O.; Thiele, R.; Åberg, G. 1988. Geochemical trends in Mesozoic Tertiary volcanic rocks from the Andes in central Chile, and tectonic implications. *Journal of South American Earth Sciences*, Vol. 1, p. 63-74.

McCulloch, M.T.; Kyser, T.K.; Woodhead, J.D.; Kinsley, L. 1994. Pb-Sr-Nd-O isotopic constraints on the origin of rhyolites from the Taupo volcanic Zone of New Zealand: evidence for assimilatioin followed by fractionation from basalt. *Contributions to Mineralogy and Petrology*, Vol. 115, p. 303-312.

Meschede, M. 1986. A method of discriminating between different types of mid-ocean ridge basalts and continental tholeiites with the Nb-Zr-Y diagram. *Chemical Geology*, Vol. 56, p. 207-218.

Middlemost, E.A.K. 1991. Towards a comprehensive classification of igneous rocks and magmas. *Earth Science Reviews*, Vol. 31, p. 73-87.

Miyashiro, A. 1974. Volcanic rock series in island arcs and active continental margins. *American Journal of Science*, Vol. 274, p. 321-355.

Mpodozis, C.; Kay, S.M. 1992. Late Paleozoic to Triassic evolution of the Gondwana margin: evidence from Chilean Frontal Cordilleran Batholiths (28°S to 31°S). *Geological Society of America, Bulletin*, Vol. 104, p. 999-1014.

Mpodozis, C.; Kay, S.M.; Nasi, C.; Moscoso, R.; Cornejo, P. 1988. Granitoides del Paleozoico-Triásico de la alta Cordillera entre los 28° y 31°S: geoquímica de elementos trazas y tierras raras. *Comunicaciones*, Vol. 39, p. 268.

Muñoz-Cristi, J. 1942. Rasgos generales de la constitución geológica de la Cordillera de la Costa especialmente en la provincia de Coquimbo. *In* Primer Congreso Panamericano de Ingeniería de Minas y Geología. *Imprenta y Litografía Universo, S.A.*, Vol. 2, p. 285-318. Santiago.

Muñoz-Cristi, J. 1973. Geología de Chile. *Editorial Andrés Bello*, 209 p.

Nakamura, N. 1974. Determination of REE, Ba, Mg, Na and K in carbonaceous and ordinary chondrites. *Geochimica et Cosmochimica Acta*, Vol. 38, p. 757-775.

Oyarzún, M.; Aguirre, L.; Morata, D. 1997. Quimismo bimodal y metamorfismo de bajo grado en las rocas volcánicas triásicas de la cordillera de la Costa de Chile central. *In Congreso Geológico Chileno, No. 8, Actas*, Vol. 2, p. 1424-1428. Antofagasta.

Parada, M.A.; Levi, B.; Nyström, J.O. 1991. Geochemistry of the Triassic to Jurassic plutonism of Central Chile (30 to 33°S); petrogenetic implications and a tectonic discussion. *Geological Society of America, Special Paper*, Vol. 265, p. 99-112.

Parada, M.A.; Nyström, J.O.; Levi, B. 1999. Multiple sources for the Coastal Batholith of central Chile (31-34°S): geochemical and Sr-Nd isotopic evidence and tectonic implications. *Lithos*, Vol. 46, p. 505-521.

Pearce, J.A. 1982. Trace element characteristics of lavas from destructive plate boundaries. *In* Andesites; orogenic andesites and related rocks (Thorpe, R.S.; editor). *John Wiley and Sons*, p. 525-548.

Pearce, J.A. 1983. Role of sub-continental lithosphere in magma series at active continental margins. *In* Continental basalts and mantle xenoliths (Hawkesworth, C.J.; Norry, M.J.; editors). *Shiva*, p. 230-249. Chesire, U.K.

Pearce, J.A.; Cann, J.R. 1973.Tectonic setting of basic volcanic rocks determined using trace element analyses. *Earth and Planetary Science Letters*, Vol. 19, p. 290-300.

Pearce, J.A.; Harris, N.B.W.; Tindle, A.G. 1984. Trace element discrimination diagrams for the tectonic interpretation of granitic rocks. *Journal of Petrology*, Vol. 25, p. 956-983.

Rickwood, P.C. 1989. Boundary lines within petrologic diagrams which use oxides of major and minor elements. *Lithos*, Vol. 22, p. 247-263.

Rivano, S.; Sepúlveda, P. 1986. Hoja Illapel. *Servicio Nacional de Geología y Minería, Carta Geológica de Chile*, No. 69, escala 1:250.000.

Rollinson, H. 1993. Using geochemical data: evaluation, presentation, interpretation. *Longman Scientific & Technical*, 352 p. London.

Sun, S.S.; McDonough, W.F. 1989. Chemical and isotopic systematics of oceanic basalts: implications for mantle composition and processes. *In* Magmatism in the Ocean Basins (Saunders, A.D.; Norry, M.J.; editors). *Geological Society of London, Special Publication*, Vol. 42, p. 313-345.

Thompson, R.N.; Morrison, M.A. 1988. Asthenospheric and lower lithospheric mantle contributions to continental extensional magmatism: an example from the British Tertiary Province. *Chemical Geology*, Vol. 68, p. 1-15.

Vergara, M.; López-Escobar, L.; Cancino, A. 1991. The Pichidangui Formation: Some geochemical characteristics and tectonic implications of the Triassic marine volcanism in central Chile (31°55' to 32°20'S). *Geological Society of America, Special Paper*, No. 265, p. 93-98.

Vergara, M.; Levi, B.; Nyström, J.O. Cancino, A. 1995. Jurassic and Early Cretaceous island arc volcanism, extension and subsidence in the Coast Range of central Chile. *Geological Society of America, Bulletin*, Vol. 107, p. 1427-1440.

Vicente, J.C. 1976. Exemple de 'volcanisme initial euliminaire': les complexes albitophyriques neotriasiques et mésojurassiques du secteur côtier des Andes Méridionales centrales (32° à 33° L. Sud) (González-Ferrán, O.; editor). *IAVCEI, In Proceedings* of the Symposium on 'Andean and Antarctic Volcanolgy Problems'. *Francesco Giannini and Figli*, p. 267-329. Napoli, Italy.

Vidal, P. 1994. Géochimie. *Dunod*, 190 p. Paris.

Zindler, A.; Hart, S.R. 1986. Chemical geodynamics. *Annuary Review of Earth and Planetary Sciences*, Vol. 14, p. 493-571.

Manuscript received: November 12, 1999; accepted: May 16, 2000.